WM-7 2:10

Proceedings of the 33rd
Conference on Decision and Control
Lake Buena Vista, FL - December 1994

Adaptive Rejection of Velocity-Ripple From Position Transducer In A Motion Control System

Yue LIU† Degang CHEN‡

† China Precision Engineering Institute for Aircraft Industry, Beijing 100076

‡ Dept. of Electrical and Computer Engineering, Iowa State University, Ames, IA 50011

Abstract

Precision motion control is a fundamental control problem that has encountered numerous applications such as machining, manufacturing, microelectronics, instrumentation, testing, etc. It is recognized that velocity ripple is a major factor affecting the precision of motion control systems. This paper studies the adaptive rejection of velocity ripple caused by the periodic errors in a inductosyn transducer. After a mathematical modeling of the transducer, two adaptive control schemes are presented that compensate the transducer errors. The closed loop adaptive systems are shown to be exponentially stable in both cases. Numerical simulations demonstrate significant reduction in the power spectra of velocity ripple.

1 Introduction

Precision Motion Control Systems have been used in numerous industrial areas for years. One of the typical applications can be found in the feed control of machine tools of the manufacturing industry, where accurate, smooth position and speed control are required for contour accuracy and small surface roughness of the products. Another important application which motivated this work is in the motion simulators and testing equipment for the calibration of inertial guidance systems and components. These simulators and testing equipment are required to provide high-performance motion control with position resolution of 0.0001 degree or better.

In the development of the precision motion control systems, various disturbances should be carefully taken into account. During the past years, many studies were done on the mechanical problems such as friction and backlash. Periodic ripple also has been found to be a major problem in precision motion control. These ripples can be caused by motors and motion transducers. In [1], Bolton *et al* investigated DC brushless motors which exhibit harmonic torque ripples. In [2], Chen and Paden studied step motors and indicated the damage from torque ripples to a robot motion control. In [3], Liu and Li studied velocity ripples from a multipole motion transducer in a speed control system and demonstrated experimental results. It is evident that these periodic disturbances must be reduced over a frequency range to avoid excitation of mechanical resonance or degradation of accuracy.

There are several methods to deal with ripple problems in the motion control systems. Improving components such as motion transducers and drivers is one method, and using high servo gain and an integrator to partially reduce the effect of disturbance is another. In recent years, the motion control problem has regained a lot of new interest due to the development of nonlinear, adaptive control and application of microprocessors in the control areas. In [4], a nonlinear adaptive state feedback was studied for the induction motor control. In [2], adaptive control of torque ripples was studied for step motor control and a dramatic 32 dB reduction of torque ripple was obtained.

In this paper, we study the adaptive rejection of velocity ripples from a position transducer in a high-performance motion control system. In the next section, a brief description of the phase-locked motion control system and the model of our motor control system with an inductosyn transducer are given. Then a PID servo control and the error equation used for adaptive controller design are presented. Two adaptive controllers are designed using the corrupted transducer output feedback. Finally numerical simulation results are given, demonstrating significant reduction of velocity ripples.

2 System Description

2.1 Description of A PLMCS

Figure 1 shows the functional block diagram of a phase-locked motion control system (PLMCS) developed for motion simulators. The system consists of a motor, a transducer (inductosyn) system, a command system and a servo controller. The command system is based on a specific microcomputer and generates a set of pulse and frequency signals(P_c and F_c) that are called motion commands. Another set of pulse and frequency signals are generated by the transducer system reflecting the motion output of the system. The phase error between phase command and system feedback is compared by the phase detector(P.D.) and then used to drive the motor through the servo controller and current amplifier.

In the ideal situation, the outputs of the motion control system, angular position θ and angular velocity $\dot{\theta}$, can be

0-7803-1968-0/94$4.00©1994 IEEE

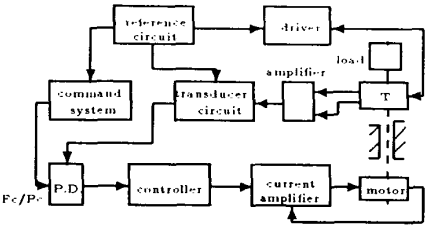

Figure 1: Block diagram of Basic PLMCS

expressed as

$$\theta = \frac{360P_c}{p_t N_r}; \quad \dot{\theta} = \frac{360F_c}{p_t N_r} \tag{1}$$

where p_t is the number of pole-pairs of the inductosyn; N_r is the resolution constant. In a well designed phase-locked motion control system, N_r can be managed in the range 1000-10000 resulting in average speed accuracy in 1-10ppm.

From test data, however, we have observed obvious periodic variational components, the velocity-ripple, in the angular speed output of the system relative to the average speed. They are much greater than the average error. By further analysis and experiments, we have found that they are from the periodic errors of the transducer system. These errors are due to the deviations of transducer circuits and the field interference as well as the structure error in the transducer system.

2.2 The Inductosyn Transducer

The motor and transducer are typically modeled together. Due to the fact that a high gain current current amplifier is used, a simplified model for the motor can be used in order to focus our attention on the transducer. Therefore, the motor dynamics are taken to be

$$\ddot{\theta} = \frac{K_t}{J} U_m = K_m U_m \tag{2}$$

where K_m is the normalized torque constant, and U_m is the control voltage.

An inductosyn is a highly accurate multipole position transducer. A rotary inductosyn consists of a disk-like rotor and a stator with printed windings. The single-phase field current in the rotor and two-phase outputs in the stator can be described by

$$U_{id}^{\tau} = i_{id}^{\tau} R_{id} + \frac{d(i_{id}^{\tau} L_{id})}{dt} \tag{3}$$

$$L_{ra} = K_{ad} sin(p_t\theta); L_{rb} = K_{bd} cos(p_t\theta) \tag{4}$$

where $U_{id}^{\tau} = [u_{ir}, u_{ia}, u_{ib}]$ is the terminal voltage in the rotor and stator windings; $i_{id}^{\tau} = [i_r, -i_a, -i_b]$ the field current and the stator output current respectively. K_{ad} and K_{bd} are amplitude constants and R_{id}, L_{id} the resistance and inductance matrices of windings. $L_{ra,b}$ are the elements of L_{id}, representing the mutual-inductance between the rotor and stator. Here the inductive reactances related to i_a and i_b can be neglected due to its properties. To derive the output equation of our inductosyn system, we denote

- ω_0 angular frequency of the energizing signal;
- ω_p fundamental frequency $p_t\dot{\theta}$, $\omega_p \leq (0.1 - 0.2)\omega_0$;
- Δ_φ phase deviation of transducer circuits;
- Δ_k magnitude deviation of the circuits;
- δ_a, δ_b electrical interference in transducer outputs;
- P error parameter vector of transducer output;
- α sum of angular errors in transducer;
- w_e periodic error vector related to p_t;
- θ_p actual angular output of transducer.

Let the input voltage of the transducer in the rotor be expressed by a complex variable $u_{ir} = K_{vr}e^{j\omega_0 t}$. By computing using equations (3) and (4), we have

$$\begin{aligned} i_r &= K_{ir}e^{j\omega_0 t} \\ u_{ia} &= K_{sa}e^{j\omega_0 t}\{j\omega_0 sin(p_t\theta) + p_t\dot{\theta}cos(p_t\theta)\} \\ u_{ib} &= K_{sb}e^{j\omega_0 t}\{j\omega_0 cos(p_t\theta) - p_t\dot{\theta}sin(p_t\theta)\} \end{aligned} \tag{5}$$

Here K_{ir} is the exciting magnitude of u_{ir}; K_{sa} and K_{sb} are the magnitude coefficients of the two outputs in the stator computed from K_{ad}, K_{bd} and K_{vr}. To obtain the measurement of system output θ, let $u_{ia}^* = ju_{ia}$ and $u_{ab} = u_{ib} + u_{ia}^*$ through the transducer circuit system. Considering the phase, magnitude deviation and field interference introduced, from Equation(5) we have the expression of u_{ia}^* and u_{ab} as

$$\begin{aligned} u_{ia}^* &= (1+\Delta_k)K_{sb}e^{j\omega_0 t}j(j\omega_0 sinp_t\theta + p_t\dot{\theta}cosp_t\theta + \delta_a)e^{j\Delta_\varphi} \\ u_{ab} &= K_{sb}jA_e e^{j(\omega_0 t + p_t\theta)} = K_{sb}jK_{ie}e^{j(\omega_0 t + p_t\theta + \alpha)} \end{aligned}$$

where A_e is the error entry due to Δ_k, Δ_φ and $\delta_{a,b}$. Disregarding higher order terms, A_e and α can be expressed as

$$\begin{aligned} A_e &= a_e + jb_e; \quad \alpha \approx \tfrac{b_e}{a_e} \\ a_e &= \omega_0 + \omega_p + (\omega_0 - \omega_p)(\tfrac{\Delta_k}{2}cos(2p_t\theta) - \tfrac{\Delta_\varphi}{2}sin(2p_t\theta)) \\ &\quad + \tfrac{\Delta_k}{2}(\omega_0 + \omega_p) + \delta_a cos(p_t\theta) + \delta_b sin(p_t\theta) \\ b_e &= (\omega_0 - \omega_p)(\tfrac{\Delta_k}{2}sin(2p_t\theta) - \tfrac{\Delta_\varphi}{2}cos(2p_t\theta)) \\ &\quad + \tfrac{\Delta_\varphi}{2}(\omega_0 + \omega_p) - \delta_a sin(p_t\theta) - \delta_b cos(p_t\theta) \end{aligned}$$

Since

$$\begin{aligned} |2(\omega_0 + \omega_p)| \gg |\Delta_k(\omega_0 + \omega_p) - \Delta_k(\omega_0 - \omega_p)cos(2p_t) \\ -\Delta_\varphi(\omega_0 - \omega_p)sin(2p_t) + \delta_a cos(p_t\theta) + \delta_b sin(p_t\theta)| \end{aligned}$$

we have the expression of output error of the transducer system as

$$\alpha = P^{\tau} w_e \tag{6}$$

Here vectors P and w_e are in the forms of

$$P = \begin{bmatrix} \frac{\Delta_\varphi}{2} \\ -\delta_a \\ -\delta_b \\ \frac{\Delta_k}{2} - \Delta_k \frac{\omega_p}{\omega_p + \omega_0} \\ -\frac{\Delta_\varphi}{2} + \Delta_\varphi \frac{\omega_p}{\omega_p + \omega_0} \end{bmatrix}; w_e = \begin{bmatrix} 1 \\ sin(p_t\theta) \\ cos(p_t\theta) \\ sin(2p_t\theta) \\ cos(2p_t\theta) \end{bmatrix} \tag{7}$$

Then the actual angular output θ_p of the inductosyn, in electrical phase, can be written as

$$\theta_p = p_t\theta + P^\tau w_e \tag{8}$$

Hence the torque motor with a inductosyn transducer is described by equations (2) and (8) together. Furthermore, it clearly indicates the existence of periodic errors in the system output. These errors cause velocity-ripple when the system is commanded to operate at a constant speed $\dot{\theta}$. The parameters represented by P are some uncertain constants for each speed $\dot{\theta}$ and the shape structure represented by w_e depends on angular position θ.

3 Servo Controller

To ensure the servo and tracking performances of the motion system, here a PID servo controller with input feed forward is used. We denote by θ_r, $\dot{\theta}_r$ and $\ddot{\theta}_r$ the input trajectory: angular position, speed and acceleration; $e_b = \theta_r - \theta p$ the nominal output error; $e_a = \theta r - p_t\theta$ the true output error; K_i, K_p and K_d the parameters of our PID controller. Then the controller is described as

$$U_m = \frac{\ddot{\theta}_r + [K_d\dot{e}_b + K_p e_b + K_i \int e_b dt]}{p_t K_m} \tag{9}$$

Substituting equation(9) into equation(2) and using the denotation of $e_{a,b}$, the error equation becomes

$$\ddot{e}_a + K_d\dot{e}_b + K_p e_b + K_i \int e_b dt = 0 \tag{10}$$

where $K_i, K_d > 0; K_d K_p > K_i$. Notice that $e_b = \theta_r - \theta p = e_a - P^\tau w_e$ includes the periodic error of the transducer. To reject the velocity-ripple caused by the transducer error, a compensation signal which is adjusted by an adaptive controller will be added at the input of PID controller. Since the constant component in the transducer error does not contribute to the velocity-ripple, the compensation signal can be determined as $u_c = \hat{P}^\tau w$, where $w^\tau = [sin(p_t\theta), cos(p_t\theta), sin(2p_t\theta), cos(2p_t\theta)]$ and $\hat{P} \in R^4$. Let $e_p = e_b + \hat{P}^\tau w$ and $\tilde{P} = \hat{P} - P$. From equation(10), we have

$$\ddot{e}_p + K_d\dot{e}_p + K_p e_p + K_i \int e_p dt = \ddot{\tilde{u}}_c \tag{11}$$

By denoting $G_p(s) = \frac{s^3}{s^3+K_d s^2+K_p s+K_i}$, we have Laplace form of (11) as $e_p(s) = G_p(s)\tilde{u}_c(s)$, where $\tilde{u}_c = \tilde{P}^\tau w$ is the residual ripple. Our purpose then is to design an adaptive controller forcing $\tilde{P}$ and $e_a \longrightarrow 0$. Although the compensation signal can be added into other places of the system, we have found that they will be equivalent for the design of the adaptive controller.

4 Adaptive Controller

Conventionally the velocity-ripple is dealt with by careful adjustments of the transducer system. Indeed, this process can be very costly. In this section, adaptive rejection will be studied. Since the true system error e_a is unavailable in the system, Lyapunov approach can not be directly used for the control design as can be done in the motor control case. We will discuss two design methods.

4.1 Augmented Error Method

4.1.1 Adaptive Controller Design

Choose a filter $L(s)$ and the augmented error e_ϵ as

$$L(s) = \frac{s^3 + as^2 + bs + c}{s^3}, e_\epsilon = e_p + e_\eta$$

Since $P \in R^4$ is constant, e_η can be written as

$$e_\eta = G_p(s)L(s)[\tilde{P}^\tau L^{-1}(s)w - L^{-1}(s)\tilde{P}^\tau w] \tag{12}$$

Then e_ϵ can be expressed as

$$e_\epsilon = G_p L\tilde{P}^\tau w_l = \frac{s^3 + as^2 + bs + c}{s^3 + K_d s^2 + K_p s + K_i}\tilde{P}^\tau w_l \tag{13}$$

where $w_l = L^{-1}(s)w$ and $L^{-1}(s)$ is stable. By denoting $\bar{z}$ as the internal variables, we have the sate space realization of (13)

$$\begin{aligned} \dot{\bar{z}} &= A_z\bar{z} + \bar{b}\tilde{P}^\tau w_l \\ e_\epsilon &= \tilde{P}^\tau w_l + \bar{h}^\tau\bar{z} \end{aligned} \tag{14}$$

and the transfer function

$$G_p(s)L(s) = d + \bar{h}^\tau(sI - A_z)^{-1}\bar{b} \tag{15}$$

Here $d = 1$. Hence consider a Lyapunov Function candidate

$$V = \bar{z}^\tau B\bar{z} + \tilde{P}^\tau\Gamma^{-1}\tilde{P} \tag{16}$$

with $B > 0$ and $\Gamma > 0$. Differentiating V along the solutions of the error equation(14) yields

$$\dot{V} = \bar{z}^\tau(A_z^\tau B + BA_z)\bar{z} + 2\tilde{P}^\tau w_l z^\tau B\bar{b} + 2\tilde{P}^\tau\Gamma^{-1}\dot{\tilde{P}}. \tag{17}$$

From equation(23), the update law should be

$$\dot{\tilde{P}} = \dot{\hat{P}} = -e_\epsilon\Gamma w_l \tag{18}$$

Since A_z is Hurwitz and $L(s)$ can always be selected such that $G(s)L(s)$ is strictly positive real(SPR), the well-known MKY Lemma [5] will yield a matrix $B = B^\tau > 0$, a scalar $v > 0$ and a vector q for a given matrix $D = D^\tau > 0$; such that

$$A_z^\tau B + BA_z = -qq^\tau - vD; \quad B\bar{b} - \bar{h} = \pm\sqrt{2}q$$

Then $\dot{V}$ can be written as

$$\dot{V} = -v\bar{z}^\tau D\bar{z} - (\bar{z}^\tau q \mp \sqrt{2}\tilde{P}^\tau w_l)^2 \tag{19}$$

Since $V > 0$ and $\dot{V} \leq 0$ for all $\bar{z}$ and $\tilde{P}$, immediately the system presented by equations (14) and (18) is stable in the sense of Lyapunov.

4.1.2 Further Analysis of The Stability

Since V is positive definite and $\dot{V}$ is nonpositive, we have V nonincreasing. Therefore, $V(t)$ —— constant as $t \longrightarrow \infty$ and $V(0) \geq V(t) \geq 0 \ \forall t > 0$, meaning that $V(t) \in L_\infty$. From equation (16), both $\bar{z}$ and $\tilde{P} \in L_\infty$, since $B > 0$ and $\Gamma^{-1} > 0$.

Next we want to use Barbalat's Lemma [6] to establish convergence of the augmented error. To do this, let's denote $L_m = \|L^{-1}\|_\infty$, since $L^{-1}(s)$ is stable. Then we have $\|w_l\| \leq L_m\|(1,1,1,1)\|$. Then $\tilde{P} \in L_\infty$ implies $\tilde{P}^\tau w_l \in L_\infty$. Therefore $\dot{\bar{z}} = A_z\bar{z} + \bar{b}\tilde{P}^\tau w_l \in L_\infty$. Furthermore, since the system is stable and $\dot{\theta}_r \in L_\infty, \dot{\theta} \in L_\infty$. Then $\dot{w} = \begin{pmatrix} 0 & 1 & 0 & 0 \\ -1 & 0 & 0 & 0 \\ 0 & 0 & 0 & 1 \\ 0 & 0 & -1 & 0 \end{pmatrix} w p_t \dot{\theta} \in L_\infty$. Hence $\dot{w}_l = L^{-1}\dot{w} \in L_\infty$. Also $\dot{\tilde{P}} = -\Gamma e_\epsilon w_l = -\Gamma(\tilde{P}^\tau w_l + \bar{h}^\tau \bar{z})w_l \in L_\infty$. With all these, we finally have $\ddot{V} = -2v\bar{z}D\dot{\bar{z}} - 2(\bar{z}^\tau q \pm \sqrt{2}\tilde{P}^\tau w_l)(\dot{\bar{z}}^\tau q \pm \sqrt{2}\dot{\tilde{P}}^\tau w_l \pm \tilde{P}^\tau \dot{w}_l) \in L_\infty$, which ensures that $\dot{V}$ is uniformly continuous. This plus $V(t) \longrightarrow$ constant as $t \longrightarrow \infty$ leads to the conclusion that $\dot{V} \longrightarrow 0$ as $t \longrightarrow \infty$. Therefore, $\bar{z}^\tau D\bar{z} + (\bar{z}^\tau \pm \sqrt{2}\tilde{P}^\tau w_l)^2 \longrightarrow 0$ as $t \longrightarrow \infty$. Both $\bar{z}^\tau D\bar{z} \longrightarrow 0$ and $\bar{z}^\tau \pm \sqrt{2}\tilde{P}^\tau w_l \longrightarrow 0$ as $t \longrightarrow \infty$. Then we have $\tilde{P}^\tau w_l, e_\epsilon \longrightarrow 0$ as $t \longrightarrow \infty$.

In order to establish the convergence of the tracking error e_p, the argument follows like this: By the swapping Lemma [6], the auxiliary error e_η is of the form $e_\eta = H(s)\dot{\tilde{P}}$ where $H(s)$ is a suitable, stable operator. Since $e_\epsilon \longrightarrow 0$ as $t \longrightarrow \infty$, equation (18) leads to $\dot{\tilde{P}} \longrightarrow 0$ as $t \longrightarrow \infty$. Therefore $e_\eta \longrightarrow 0$ as $t \longrightarrow \infty$. This immediately leads to $e_p = e_\epsilon - e_\eta \longrightarrow 0$ as $t \longrightarrow \infty$.

Moreover, for our adaptive control system, we can achieve stronger stability results: the exponential convergence of tracking error and parameters. This is obtained by establishing persistence of excitation(PE) of the regressor w_l and by ensuring that $G_p(s)L(s)$ is SPR. Since the system is stable, we can easily ensure that $\dot{\theta}_M \geq |\dot{\theta}| \geq \dot{\theta}_m > 0$ by proper choice of the reference trajectory. This is an easy task, since in practice the motor will be rotating at a nearly constant speed. Then by the PE Lemma of [2], w will be PE; and therefore w_l is PE since $w_l = L^{-1}(s)w$ and L^{-1} is stable. To ensure that $G_p(s)L(s)$ is SPR, one can show that if we choose a, b, c such that $aK_d > b + K_p; bK_p > cK_d + aK_i; c > 0$, then $Re[G_p(jw)L(jw)] > 0 \ \ \forall\omega \in R$. Since the relative degree of $G_p(s)L(s)$ is zero, the above guarantees that $G_p(s)L(s)$ is SPR [5]. Then using the standard results of stable adaptive systems [7], we conclude $\bar{z}$ and $\tilde{P} \rightarrow 0$ exponentially as $t \rightarrow \infty$; So does e_ϵ and e_a.The velocity-ripple will be rejected as $\tilde{P}^\tau w \longrightarrow 0$.

4.2 Averaging Method

In simulation, we observed the instability of the system when using e_p as the input to the adaptive controller for some output speed. This motivates the use of the averaging methods [8] [7] to analyze the properties of the adaptive system and hence leads to an alternative design of the controller.

Considering the parameter adaptation in the form of equation (18) and pretending to use ϵ_p in place of ϵ_ϵ, we have

$$\dot{\tilde{P}} = \dot{P} = -e_p\Gamma w \tag{20}$$

It can be verified that $e_p(t)$ can be expressed as

$$e_p(t) = -\int_0^t G_1(t-\tau)\tilde{P}^\tau(\tau)w(\tau)d\tau + \tilde{P}^\tau w \tag{21}$$

where $G_1(s) = 1 - G_p(s) = \frac{K_d s^2 + K_p s + K_i}{s^3 + K_d^2 + K_p s + K_i}$. To derive the averaging equation for (21), we write the regression vector w in the Fourier form

$$w^\tau(t) = [sin(p_t\theta), cos(p_t\theta), sin(2p_t\theta), cos(2p_t\theta)] \tag{22}$$

$$= \sum_{n=-2, n\neq 0}^{n=2} C_n e^{j\omega_n t} \tag{23}$$

where C_n are Fourier coefficients and ω_n can be written as $2n\pi\dot{\theta}$ approximately[3]. Then the averaging equation for parameter adaptation can be described as[8] [7]

$$\dot{\bar{P}}_{av} = -\Gamma\bar{Q}\bar{P}_{av} \tag{24}$$

where

$$\bar{Q} = \frac{1}{T}\int_0^T (-w(t)\sum G_1(j\omega_n)C_n^\tau e^{j\omega_n t} + ww^\tau)dt$$

$$= \sum G_p(j\omega_n)C_nC_{-n}^\tau$$

Since w is PE $\Longrightarrow \sum ReC_nC_{-n}^\tau > 0$. But $G_p(s)$ is not SPR. In fact, we have

$$G_p(j\omega) = \frac{-j\omega^3(K_i - K_d\omega^2) - \omega^3(K_p\omega - \omega^3)}{(K_i - K_d\omega^2)^2 + (K_p\omega - \omega^3)^2}$$

$$Re[G_p(j\omega)] < 0 \tag{25}$$

or $\omega^2 < K_p$, *i.e.*, there exist eigenvalues with positive real parts in the system (24),for some $\omega_n^2 < K_p$. In other words, the phase of $G_p(j\omega)$ was shifted out of the range $\pm\frac{\pi}{2}$.

Based on this fact, we rewrite the transfer function $G_p(j\omega)$ as

$$G_p(j\omega) = jIm[G_p(j\omega)] + Re[G_p(j\omega)] = |G_p(j\omega)|e^{j\beta(\omega)} \tag{26}$$

and let the regression vector in the parameter adaptation (21) be $w_p = B_p w$, obtained by changing the phase of the regressor w, where

$$B_p = \begin{bmatrix} e^{j\alpha_{p1}(\omega_n)} & 0 & 0 & 0 \\ 0 & e^{j\alpha_{p1}(\omega_n)} & 0 & 0 \\ 0 & 0 & e^{j\alpha_{p2}(\omega_n)} & 0 \\ 0 & 0 & 0 & e^{j\alpha_{p2}(\omega_n)} \end{bmatrix}.$$

Then the pretending parameter adaptation law is corrected to be

$$\dot{\tilde{P}} = -e_p\Gamma w_p \tag{27}$$

The modified averaging equation for the parameter update law of (28) can be expressed as

$$\dot{\tilde{P}}_{av} = -\Gamma \bar{Q}_p \tilde{P}_{av}, \tag{28}$$

where

$$\bar{Q}_p = \sum |G_p(j\omega_n)| e^{j q_n(\omega_n)} C_n C_{-n}^{\tau} \tag{29}$$

with $q_{1,2}(\omega_n) = \beta(\omega_n) + \alpha_{p1,2}(\omega_n)$. Then $\alpha_{p1,2}(\omega)$ are selected such that $|q_{1,2}(\omega_n)| < \frac{\pi}{2}$. By general results of slow adaptive system in the averaging analysis, the system presented by the equations (16) with the parameter adaptation (34) and modified phase $q_{1,2}(\omega_n)$ will be exponentially stable. Hence we have $\tilde{P} \to 0, e_p \to 0$ and consequently $e_a \to 0$ as $t \to \infty$.

On the other hand, because θ is unavailable, the trajectory θ_r will be used in the regressor. We denote $w_r^{\tau} = [sin(\theta_r), cos(\theta_r), sin(2\theta_r), cos(2\theta_r)]$. Substituting $\theta_r = p_t\theta + e_a$ into w_r, we have

$$\hat{P}^{\tau} w_r - P^{\tau} w = \tilde{P}^{\tau} w_r + P^{\tau} E_a w_r$$

where $E_a =$

$$\begin{bmatrix} 1-cos(e_a) & sin(e_a) & 0 & 0 \\ -sin(e_a) & 1-cos(e_a) & 0 & 0 \\ 0 & 0 & 1-cos(2e_a) & sin(2e_a) \\ 0 & 0 & -sin(2e_a) & 1-cos(2e_a) \end{bmatrix}.$$

Since $P^{\tau} E_a w_r$ are bounded, the parameter error $\tilde{P}$ will converge to a neighborhood of $\|P^{\tau} E_a w_r\|$. In general, the transducer error is small.

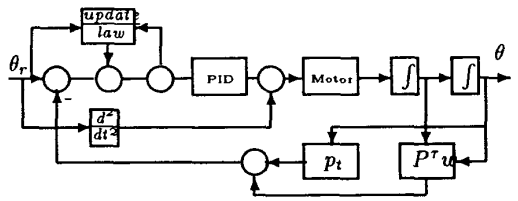

Figure 2: Block diagram of the adaptive system

5 Numerical Simulation Results

Our system is shown in Figure 2. To verify the designs and our analysis, both adaptive controllers are studied in the simulation work. The ripple spectra and parameter dynamics were calculated and recorded. Based on an actual phase-locked motion control system with the position transducer-inductosyn developed for gyro tests, the following parameters are used to analyze the system performance in the simulation.

$$J = 3149.7(g.cm.s^2); \quad K_t = 0.22(Kg(f).m/A);$$
$$p_t = 360; \quad N_r = 2500;$$
$$\omega_0 = 4000 \times 2\pi(rad/s); \quad max(\omega_p) = 0.2\omega_o;$$

The total angular error of the transducer system is estimated to be 11 arc seconds. The deviation coefficients in phase, magnitude and field interference are chosen as

$$\Delta_k = 6.23 \times 10^{-3} \quad \Delta_\varphi = 6.23 \times 10^{-3}$$
$$\delta_a = 5.24 \times 10^{-3} \quad \delta_b = 5.24 \times 10^{-3}$$

They are equivalent to about 0.36 and 0.3 electrical degree respectively that are used in the simulation.

For the PID servo controller, $K_i = 22$; $K_p = 550$; $K_d = 110$ were chosen. Frequency bandwidth(-3dB) is about $20Hz$. Small overshoot was achieved.

Figure 3 illustrates the power spectral density(PSD) of the velocity ripples caused by the periodic error of the transducer system without any adaptive rejection when $\dot{\theta}_r = 2$ degree per second(deg/s).

Figure 4 to Figure 6 show the simulation results of adaptive ripple rejection of the augmented error design with $\dot{\theta}_r = 2$ deg/s. Figure 4 shows the rejected velocity-ripple spectra (PSD); Figure 5 the time history of $\dot{\theta}$ (deg/s); Figure 6 the convergence of one parameter corresponding to the term $sin(\theta_r)$ from an initial value of 0 electrical degree(deg). In filter $L(s)$, the parameters are chosen as $a = 55$, $b = 275$, $c = 10$. Notice that the ripple spectra(PSD) has been reduced significantly.

Figure 7 to Figure 9 show the results using averaging analysis design method at nominal motor speed of 2 deg/s. Figure 7 and Figure 8 are spectra(PSD) and time history (deg/s); Figure 9 and Figure(10) the convergence of two parameters corresponding to $sin(\theta_r)$ and $sin(2\theta_r)$ respectively. The initial values are both zeros. $\beta(\omega)$ is compensated by $\alpha_p(\omega)$ such that $q_n(\omega)$ in the range of $\pm\frac{\pi}{4}$. Notice again the dramatic reduction in the velocity-ripple spectra(PSD).

6 Conclusion

Periodic ripple is one of the major errors greatly damaging the performance of precision motion control systems. Our work shows the generation of the velocity-ripple from a position transducer-inductosyn and the adaptive rejection of those ripples. Since the true output of the system can not be available in transducer case, two stable controllers are studied. In particular, the controller designed by averaging analysis is much easier to be implemented by numerical control. Compensation phase α_p can be determined by the frequency response of the system. Simulation results demonstrated that velocity-ripples are reduced to significantly. Experimented work will be developed in the future. Moreover, the simplicity of adaptive ripple rejection may lead to significant economic benefit over manual adjustment of the transducer. The controller developed here may be further applied to other applications which encounter ripple problems.

Figure 3 frequency(Hz)

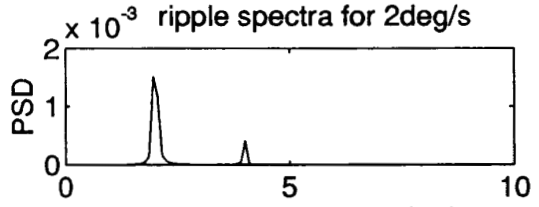

Figure 4 frequency(Hz)

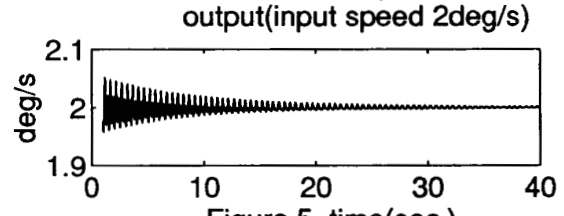

Figure 5 time(sec.)

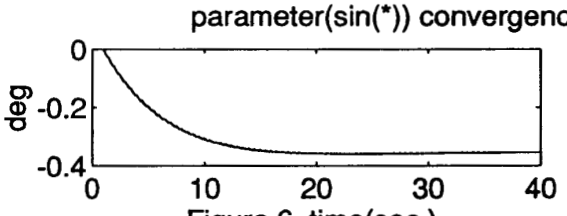

Figure 6 time(sec.)

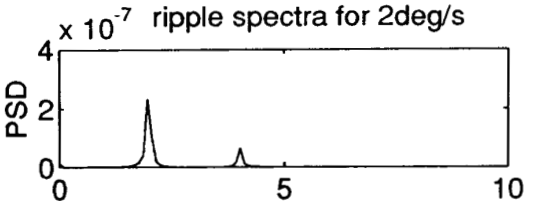

Figure 7 frequency(Hz)

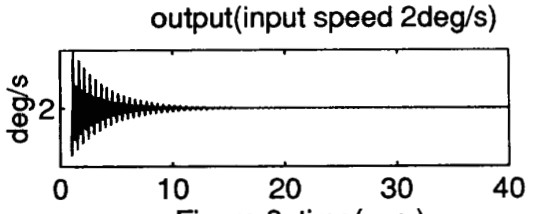

Figure 8 time(sec.)

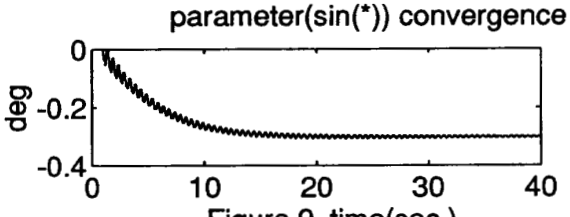

Figure 9 time(sec.)

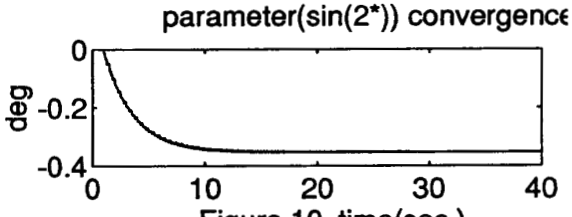

Figure 10 time(sec.)

References

[1] Bolten, Ashen, "Influence of Motor Design and Current Waveforms on Torque Ripple in Brushless DC Driver", Proc. IEE, Pt. B 131 pp.82-90 1984.

[2] Degang Chen and Brad Paden, "Nonlinear Adaptive Torque-Ripple Cancelation for Step Motor", CDC pp.3319-3324 1990.

[3] Liu Yue and Li Yia-jun, "Experiment Analysis of Velocity-Ripple in Rate Test Tables", China Precision Manufacturing Engineering for Aircraft Industry, No.8 1990.

[4] R.Marino, S.Peresada and P.Valigi, "Adaptive Partial Feedback Linearization of Induction Motors", Proc. of IEEE CDC, 1990. pp127-160.

[5] Narendra and M.Aunaswamy, "Stable Adaptive Control System" Prentice Hall, Englewood Cliffs, New Jersey, 1989.

[6] S.Sastry and M.Bodson, "Adaptive Control, Stabilities, Convergence and Robustness", Prentice Hall, Englewood Cliffs, New Jersey,1989.

[7] B.D.O.Anderson, R.R.Bitmead, C.R.Johnson,Jr., P.V.Kokotovic, R.L.Kosut, I.M.Y.Mareels, L.Praly and B.D.Riedle, "Stability of Adaptive Systems" The MIT Press, Cambridge, Massachusetts, 1986.

[8] Bradly D.Riedle and Petar V.Kokotovic, "Stability-Instability Boundary for Disturbance-Free Slow Adaptation with Unmodeled Dynamics" IEEE Trans. on Automatic Control, Vol. AC-30 No.10 pp.1027-1030 1985.